PROCEEDINGS OF SPIE

SPIEDigitalLibrary.org/conference-proceedings-of-spie

Design of SOI wavelength filter based on multiple MMIs structures

Youfang Hu, Frédéric Gardes, Richard Jenkins, Ewan Finlayson, Goran Mashanovich, et al.

Youfang Hu, Frédéric Y. Gardes, Richard M. Jenkins, Ewan D. Finlayson, Goran Z Mashanovich, Graham T. Reed, "Design of SOI wavelength filter based on multiple MMIs structures," Proc. SPIE 7943, Silicon Photonics VI, 79430X (27 January 2011); doi: 10.1117/12.875280

SPIE.

Event: SPIE OPTO, 2011, San Francisco, California, United States

Design of SOI wavelength filter based on multiple MMIs structures

Youfang Hu*, Frédéric Y. Gardes, Richard M. Jenkins, Ewan D. Finlayson,
Goran Z. Mashanovich, Graham T. Reed
Advanced Technology Institute, University of Surrey, Guildford, GU2 7XH, UK

ABSTRACT

SOI based MMIs prove to be versatile photonic structures for optical power splitting/combining, directional coupling, wavelength multiplexing/demultiplexing, etc. Such a structure benefits from relative ease of fabrication, low sensitivity to fabrication error and low temperature dependence. Whilst the majority of previous designs and optimizations investigated single MMIs, there is significant potential to combine MMIs within a single device for the realization of improved device performance. We have designed and simulated a wavelength filter device consisting of a series of MMIs with different lengths. The bandwidth, free spectral range, and extinction ratio can be controlled by changing the MMI's width and length. We have optimized our design to achieve a -3dB bandwidth of 5nm, a free spectral range of 60nm, an extinction ratio of >30dB, and a side peak suppression ratio of >22dB. Such a device can be used for high performance coarse wavelength filtering. The whole structure can fit into a 70μm×300μm area. Temperature sensitivity of the designed structures was also investigated.

Keywords: SOI, multimode interferometer, cascaded, filter, wavelength multiplexing

1. INTRODUCTION

Multimode interferometers (MMIs) have been used for a large variety of silicon photonic devices, including power splitters/combiners[1], couplers[2], switches[3], and multiplexers[4]. MMI based devices are very suitable for practical use, largely due to their relative ease of fabrication, low sensitivity to fabrication error, and low dependence on temperature, wavelength and polarization. Whilst great effort has been made to design devices based on single MMIs, there is significant potential to combine MMIs within a single device for the realization of improved device performance, e.g. higher extinction ratio, narrower wavelength bandwidth, and larger free spectral range (FSR). We have designed and simulated a wavelength filter based on cascaded MMIs. The optimized design has a -3dB bandwidth of 5nm, a free spectral range of 60nm, and an extinction ratio of >20dB. The multiple MMIs in the filter can either be arranged in line or in a wind-up style to fit in an area of 70×300μm.

2. DESIGN OF SINGLE MMI AS A FILTER

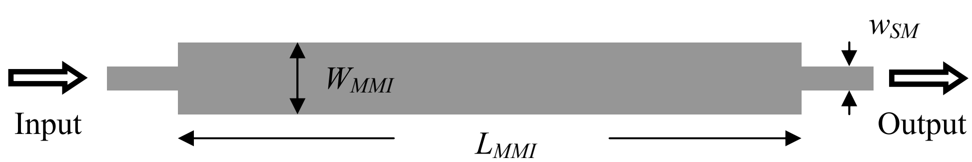

(a)

*email: y.hu@surrey.ac.uk, phone: +44 1483 68 9831

Silicon Photonics VI, edited by Joel A. Kubby, Graham T. Reed, Proc. of SPIE Vol. 7943,
79430X · © 2011 SPIE · CCC code: 0277-786X/11/$18 · doi: 10.1117/12.875280

(b) (c)

Fig. 1. Design of single narrow and long 1×1 MMI. (a) top view; (b) cross section view of single-mode waveguide; (c) cross section view of multi-mode waveguide.

Fig. 1. shows a single 1×1 MMI with one single-mode input and one single-mode output waveguide joining the multimode waveguide at the mid-point across the width of the single-mode/multimode waveguide interface. Under the geometric limitations of the configuration considered, only symmetric modes are excited in the multimode waveguide. In this MMI, the single-mode waveguide has a width of w_{SM} and the multimode waveguide has a width of W_{MMI} and a length of L_{MMI}. Suppose the device has a refractive index of n_r in the core and n_c in the cladding at the operating wavelength, λ, the 2-D approximation of the self-image distance, L_{si}, for the fundamental TE mode input is given by[5]:

$$L_{si} = \frac{p n_r W_{eff}^2}{\lambda} \text{ with } p = 0,1,2,... \tag{1}$$

where, λ is the operating wavelength, p represents the order of the self-image, and W_{eff} is the effective multimode waveguide width given by:

$$W_{eff} = W_{MMI} + \frac{\lambda}{\pi\sqrt{n_r^2 - n_c^2}} \tag{2}$$

It is obvious from equation (1) that the self-image distance, L_{si}, is linearly dependant on operating wavelength λ, and is more sensitive to wavelength change at higher self-image order, i.e. large value of p. Hence, for a fixed multimode waveguide length, L_{MMI}, the wavelength corresponding to different self-image order, p, appears periodic. Noting that the device's output has almost full transmission when the multimode waveguide has a self-image length, the transmittivity of the device can be modulated by varying the input wavelength, with the transmission maxima appearing periodically.

A commercial simulation tool, FIMMWAVE[6], based on the 3-D eigen-mode expansion method was used to model this device. Fig. 2(a) shows the field profile of a single MMI with fundamental TE mode input. It has a width of W_{MMI}=1.5μm and a length of L_{MMI}=98.3μm, which corresponds to the 21st order self-image distance at λ=1.55μm. As the MMI has a small width, the multimode waveguide only supports very few (3-4) guided modes and the MMI's self-image distance has a very short period. The field profile also shows that the fidelity of self-imaging varies with the self-image order. Indeed, such a change in fidelity corresponds to a beating of the modulation depth in the curve of transmittivity versus MMI length (Fig. 2b). Here, for a fixed wavelength, self-imaging with the best fidelity appears at a period of L_p along the MMI length. In order to achieve best performance, only MMIs with lengths of $L_{MMI}=mL_p$ (m=1,2,3,…) are considered in our design. Fig. 2(c) shows the simulated transmission spectra of the device with MMI lengths fixed at $L_{MMI}=L_p$, $2L_p$, and $3L_p$. It is evident that free spectral range is inversely proportional to L_{MMI}, and the spectral bandwidth decreases as L_{MMI} increases. It is shown that the single MMI itself may work as a coarse wavelength filter. Moreover, the filter's performance can be substantially improved with the design of multiple cascaded MMIs, which is described in the next section.

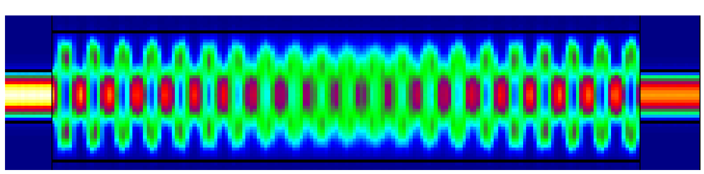

(a)

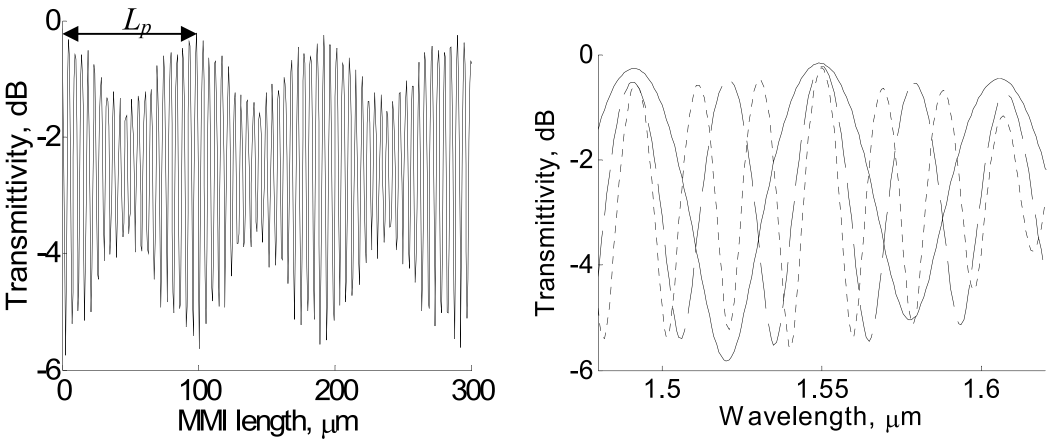

(b) (c)

Fig. 2. (a) Field profile of single 1×1 MMI (λ=1.55μm, W_{SM}=0.6μm, W_{MMI}=1.5μm, L_{MMI}=98.3μm). (b) Transmittivity as a function of L_{MMI} of the device shown in (a) (λ=1.55μm, L_p=98.3μm). (c) Transmission spectrum of the device shown in (a), at MMI lengths of $L_{MMI}=L_p$(solid curve), $L_{MMI}=2L_p$(dashed curve), $L_{MMI}=3L_p$(dotted curve).

3. DESIGN OF CASCADED MMI FILTER

High performance wavelength filters require larger free spectral range, narrow spectral bandwidth, and high extinction ratio, which is difficult to achieve using a single 1×1 MMI device, as is shown in Fig. 2. However, there is flexibility to reshape the device's spectral response by connecting multiple 1×1 MMIs in series. The spectral response, S_c, of such a filter with N MMIs is simply given by:

$$S_c = \prod_{i=1}^{N} S_i$$

where, S_i is the spectral response of the ith MMI.

Now, our design work aims to optimize the combination of multiple cascaded 1×1 MMIs, by monitoring the product of the whole device's spectral responses, so as to achieve a transmission spectrum with high extinction ratio, narrow spectral bandwidth, and large free spectral range. As this is an initial design, we only consider the situation in which each single 1×1 MMI has the same MMI width, W_{MMI}=1.5μm, the same single mode waveguide width, w_{SM}=0.6μm, but variable MMI length, L_{MMI}. The variation of W_{MMI} and w_{SM} gives another two degrees of freedom for optimization, but that is not discussed in this paper.

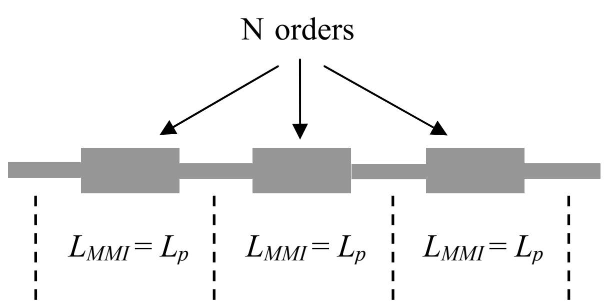

(a)

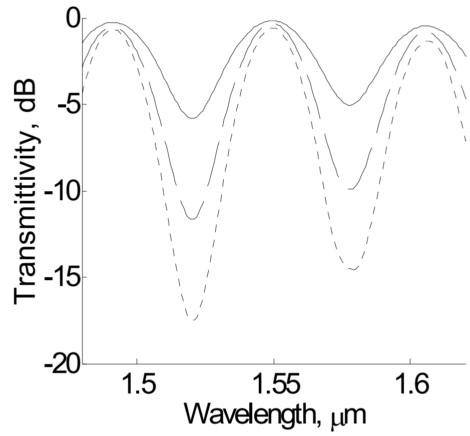

(b)

Fig. 3. Multiple (N) order cascaded MMI filter. All multimode waveguides are identical (W_{MMI}=1.5μm, L_{MMI}=L_p=98.3μm). (a) Top view layout (b) Transmission spectrum for N=1 (solid curve), N=2 (dashed curve), and N=3 (dotted curve).

Fig. 3 shows the structural layout and simulated spectral responses of cascaded 1×1 MMIs with the same length (L_{MMI}=L_p=98.3μm), as is referred to as a multiple order cascaded structure. It is evidently shown that, as the order number, N, increases, the extinction ratio increases efficiently (6-7dB per order) and the spectral bandwidth is reduced, whilst the free spectral range is not affected. The insertion loss, α_c, at the central wavelength (λ=1.55μm) is kept low for a small order number (α_c <1dB for N<=3).

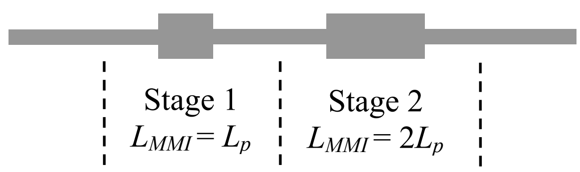

(a)

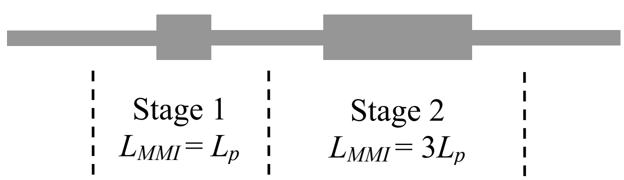

(b)

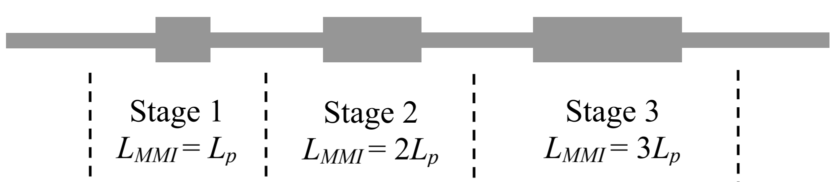

(c)

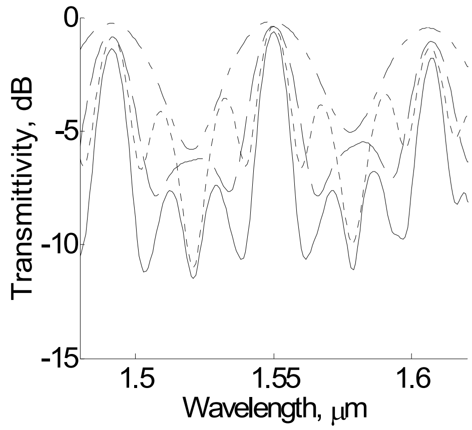

(d)

Fig. 4. Multiple stage cascaded MMI filter. Top view of three different layouts (a), (b), (c) and (d) transmission spectra for layout (a) (dashed curve), layout (b) (dotted curve), layout (c) (solid curve), and single MMI (L_{MMI}=L_p=98.3μm, dash-dotted curve).

Fig. 4 shows the structural layouts and simulated spectral responses of cascaded 1×1 MMIs with different lengths, L_{MMI}, as is referred to as a multiple stage cascaded structure, compared with single MMI (dash-dotted curve). The 1×1 MMI lengths are different at different stages and there is only one MMI in each stage. Such a multiple stage structure gives substantial reduction of spectral bandwidth, while keeping the free spectral range the same as a single 1×1 MMI. The increase of the extinction ratio is also shown, although it is not as efficient as the multiple order structure (Fig. 3) and some side peaks are visible. The three-stage structure (Fig. 3c) has the optimized spectral response (solid curve in Fig. 4d) with a -3dB spectral bandwidth of 10nm, an extinction ratio of 10dB, a side peak suppression ratio of 7dB, and a free spectral range of 60nm.

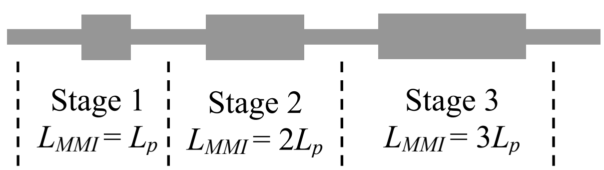

(a)

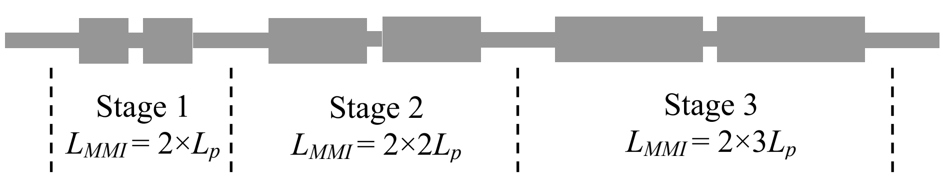

(b)

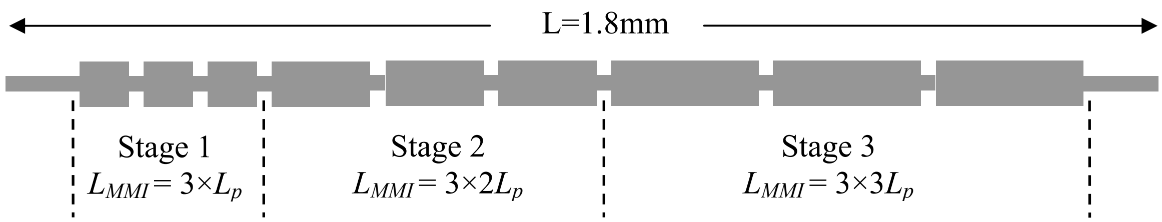

(c)

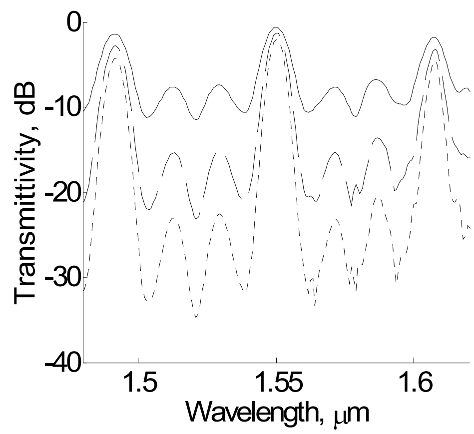

(d)

Fig. 5. Three-stage, multiple order cascaded MMI filter. (a), (b), (c) Top view of three different layouts and (d) transmission spectra for layout (a) (solid curve), layout (b) (dashed curve), and layout (c) (dotted curve).

Although the three stage structure shown in Fig. 4(c) already has a large free spectral width (60nm), for the purpose of coarse wavelength multiplexing/demultiplexing, it will be ideal to further increase the extinction ratio and side peak suppression ratio and to further reduce the spectral bandwidth. Fig. 5 shows one solution to this issue by using a three-stage design with multiple order structures in each stage. The spectral response for a three-stage, third-order cascaded MMI filter (Fig. 5c) has an extinction ratio of 30dB, a side peak suppression ratio of 22dB, and a -3dB spectral bandwidth of 5nm, while the insertion loss is kept low (α_c<3dB). Such a filter's spectral response may be further enhanced by using even higher order design, however, the length of the whole structure will exceed 2mm and insertion loss will further increase.

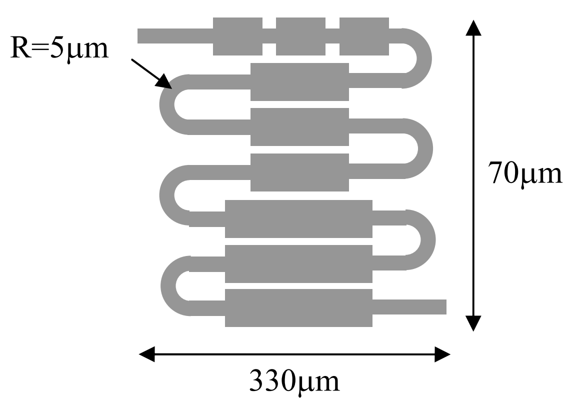

Fig. 6. Wind-up design of three-stage third-order cascaded MMI filter.

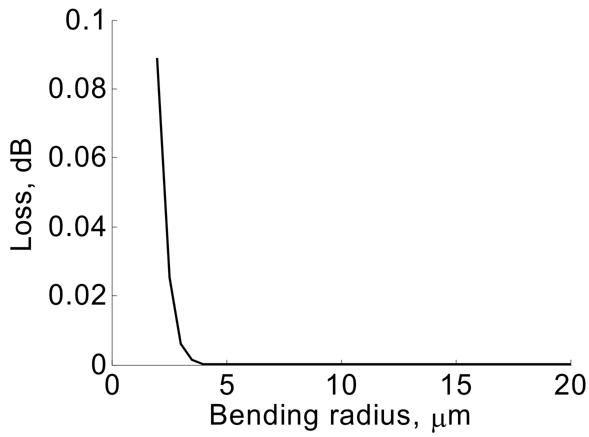

Fig. 7. 90^o bending loss of single mode waveguide structure shown in Fig. 1(b)

Fig. 6 shows the wind-up layout of the three-stage, third-order cascaded MMI filter, corresponding to the device with an in-line design shown in Fig. 5(c). It is possible to minimize the bending radius, *R*, of the single-mode waveguide, so that the footprint of the whole structure is small whilst the bending loss is kept low. Simulation using FIMMWAVE (Fig. 7) shows *R*=5μm gives negligible bending loss and it will enable the whole wind-up structure to fit into an area of 70μm by 330μm. Furthermore, this approach is also flexible enough to wind the whole structure into different shapes if required, for the purpose of integration, and maximum space utilization.

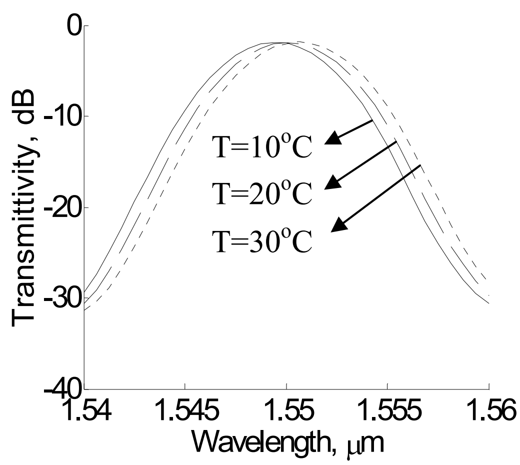

Fig. 8. Simulated transmission spectra (near transmission peak) of three-stage, third-order cascaded MMI filter at different temperatures.

In general, MMI based devices have the advantage of low sensitivity to temperature change. However, our design of the filter uses narrow and long MMIs with a length of large self-image order (integer multiple of 21st order) arranged in a cascaded style. It may have increased sensitivity to temperature change compared with conventional MMI based devices having a length of only 1st or multiple folds of 1st self-image order[1-4]. Simulation with FIMMWAVE (Fig. 8) shows the three-stage, third-order cascaded MMI filter (Fig. 5c) has a red shift of 60pm/^{o}C as the temperature increases, while there is no significant drop of peak transmittivity within a temperature range of 10^{o}C<*T*<30^{o}C. Its temperature sensitivity is comparable with the ring resonator without overlaying a polymer cladding (dλ/dT=54.2pm/^{o}C; FSR=6nm) reported in [7]. However, our filter's free spectral range is one order of magnitude wider (60nm). For the application of coarse wavelength multiplexing/demultiplexing, the influence of the same amount of temperature sensitivity (dλ/dT) to device performance is less severe in our case.

4. CONCLUSION

In conclusion, we have designed and simulated a novel wavelength filter based on a structure of multiple cascaded 1×1 MMIs. In order to prove the principle, our design was simplified by fixing all the MMIs' multimode waveguide widths at W_{MMI}=1.5μm and single mode waveguide widths at w_{SM}=0.6μm. Only the MMI length, L_{MMI}, is variable. Simulation shows that a three-stage, third-order cascaded structure has an optimized spectral response with a free spectral range of 60nm, an extinction ratio of >30dB, a side peak suppression ratio of >22dB, and -3dB spectral bandwidth of 5nm. It is ideal for the application of coarse wavelength multiplexing/demultiplexing. The whole structure can be designed in line or be arranged in a wind-up style and has the flexibility to be reshaped for the purpose of integration. Its temperature sensitivity compared with ring resonator is also investigated.

REFERENCES

[1] D. J. Thomson, Y. Hu, G. T. Reed, and Jean-Marc Fedeli, "Low Loss MMI Couplers for High Performance MZI Modulators," IEEE Photonics Technology Letters, 22(20), 1485-1487 (2010).

[2] M. K. Chin, C. L. Xu, and W. P. Huang, "Theoretical approach to a polarization insensitive single-mode microring resonator," Optics Express, 12(14), 3245-3250 (2004).

[3] F. Wang, J. Yang, L. Chen, X. Jiang, and M. Wang, "Optical switch based on multimode interference coupler," IEEE Photonics Technology Letters, 18(2), 421-423 (2006).

[4] S. L. Tsan, H. C. Guo, and C. W. Tsai, "A novel 1×2 single-mode 1300/1550 nm wavelength division multiplexer with output facet-tilted MMI waveguide," Optics Communications, 232, 371-379 (2004).

[5] L. B. Soldano and E. C. M. Pennings, "Optical multi-mode interference devices based on self-imaging: principles and applications," Journal of Lightwave Technology, 13(4), 615-627 (1995).

[6] http://www.photond.com.

[7] J. Teng, P. Dumon, W. Bogaerts, H. Zhang, X. Jian, X. Han, M. Zhao, G. Mortheir, and R. Baets, "Athermal silicon-on-insulator ring resonators by overlaying a polymer cladding on narrowed waveguides," Optics Express, 17(17), 14627-14633 (2009).